Notes on Theory and Experimental Conditions Behind Two-Photon Excitation Microscopy

ALESSANDRO ESPOSITO,[1–3] FEDERICO FEDERICI,[1,2] CESARE USAI,[1,4] FABIO CANNONE,[5,6] GIUSEPPE CHIRICO,[5,6] MADDALENA COLLINI,[5,6] AND ALBERTO DIASPRO[1,2]*

[1]*Laboratory for Advanced Microscopy, Department of Physics, University of Genoa, 16146 Genoa, Italy*
[2]*Istituto Nazionale per la Fisica della Materia, Department of Physics, University of Genoa, 16146 Genoa, Italy*
[3]*CELL BIOPHYSICS Group, European Neuroscience Institute, Göttingen 33 37073, Germany*
[4]*National Research Council, Institute of Biophysics, 16149 Genoa, Italy*
[5]*Laboratory for Advanced Bio-Spectroscopy and Department of Physics, University of Milano Bicocca, 20126, Milano, Italy*
[6]*INFM and Department of Physics, University of Milano Bicocca, 20126, Milano, Italy*

KEY WORDS two-photon excitation; fluorescence emission; optical sectioning effect

ABSTRACT This report deals with the fundamental quantum physics behind two-photon excitation also providing a link to the experimental consequences exploited in microscopy. The optical sectioning effect is demonstrated as well as the distribution of excitation and of fluorescence emission. *Microsc. Res. Tech. 63:12–17, 2004.*

INTRODUCTION

The two-photon excitation (TPE) process is a quantum phenomenon theoretically predicted by Maria Göppert-Mayer in 1931. This non-linear quantum process has had many applications in different branches of the experimental sciences. Figure 1 reproduces the first page of Göppert-Mayer's fundamental study (Göppert-Mayer, 1931).

Despite the theoretical background that has been known since 1931, two-photon microscopy (TPM) has undergone a deep and wide evolution only after the contribution of Denk and colleagues (1990). Thanks to many meaningful improvements, TPM is a very promising technique for the fields of biophysics, biology, bio-engineering, material sciences, and medicine (Diaspro, 1999, 2001; Diaspro and Chirico, 2003; Masters, 2002; Pawley, 1995; Periasamy and Diaspro, 2003).

In what follows, details that make TPE an intrinsically confocal technique will be presented, allowing for a reduction in some of the drawbacks of the one-photon excitation confocal microscopy such as photobleaching, phototoxicity, and chromatic aberrations.

INTENSITY SQUARE DEPENDENCE VERSUS POWER AND OPTICAL SECTIONING

When the interaction between light and molecules is not too "strong," the methods of perturbation theory can be applied. According to this approach, the full Hamiltonian has been split (Loudon, 1983; Nakamura, 1999; Sakurai, 1985) into a perturbation-free, time-independent H_0 and a time-dependent perturbation V:

$$H = H_0 + V \tag{1}$$

where H is very close to the unperturbed Hamiltonian H_0. We can examine the contribution of the electromagnetic interaction at the various order in V. Let the system have only two states, $|i\rangle$ and $|f\rangle$, eigenstates of time-independent H_0. The transition probability between $|i\rangle$ and $|f\rangle$ can be evaluated in terms of the time evolution operator U as:

$$W_{i\to f} = |\langle f|U(t)|i\rangle|^2 \tag{2}$$

where U can be expressed as a function of V (D-labelled operators) as:

$$U_D(t,\,0) = I + \sum_{n=1}^{\infty} \left(\frac{1}{i\hbar}\right)^n \int_0^t dt_n \int_0^{t_n} dt_{n-1} \cdots \int_0^{t2} dt_1 V_D(t_n) V_D(t_{n-1}) \cdots V_D(t_1) \tag{3}$$

$$U = U_0 U_D; \quad V_D = U_0^+ V U_0; \quad U_0 = e^{-i(H_0/h)t} \tag{4}$$

The transition probability can thus be estimated at different orders out of equations (3) and (4). The zero-order correction leads to null probability of transition between $|i\rangle$ and $|f\rangle$, owing to the orthogonality property of eigenfunctions. On the contrary, it can be shown that the first order transition probability is proportional to the matrix element:

$$|V_{fi}|^2 = |\langle f|V|i\rangle|^2 \tag{5}$$

that is again proportional to the single-photon absorption cross-section.

The choice of wavelengths in TPE applications is typically performed to get the single-photon cross-section negligible. This allows the calculation of a second order transition probability:

*Correspondence to: Alberto Diaspro, LAMBS, Department of Physics, University of Genoa, Via Dodecaneso 33, 16146 Genoa, Italy.
E-mail: diaspro@fisica.unige.it

Received 10 August 2003; accepted in revised form 29 September 2003
DOI 10.1002/jemt.10425
Published online in Wiley InterScience (www.interscience.wiley.com).

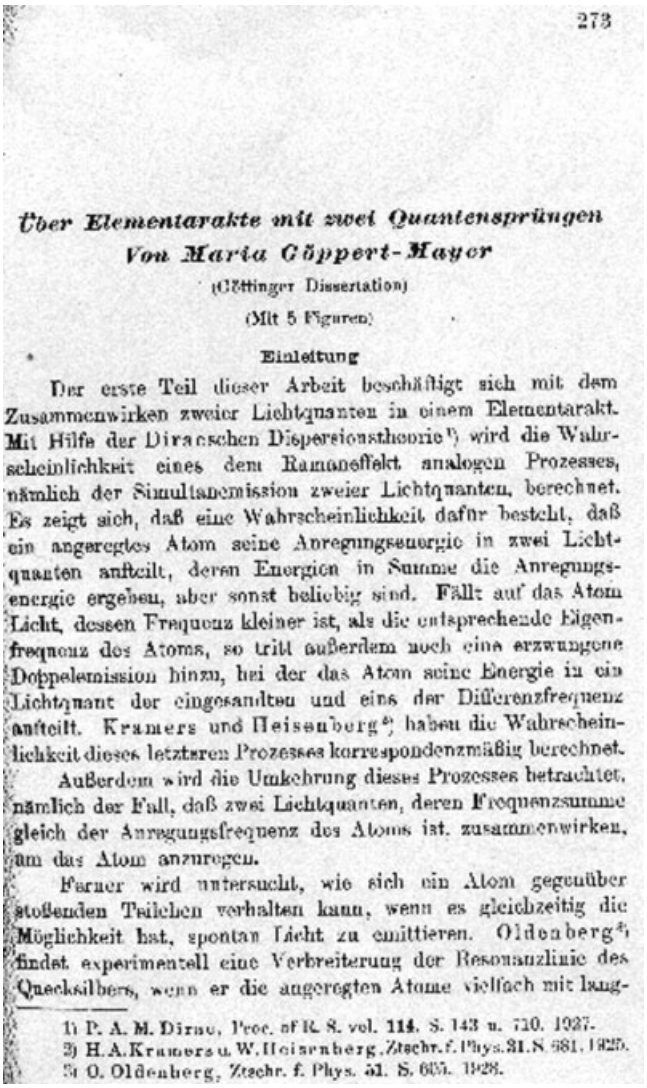

273

Über Elementarakte mit zwei Quantensprüngen

Von Maria Göppert-Mayer

(Göttinger Dissertation)

(Mit 5 Figuren)

Einleitung

Der erste Teil dieser Arbeit beschäftigt sich mit dem Zusammenwirken zweier Lichtquanten in einem Elementarakt. Mit Hilfe der Diracschen Dispersionstheorie[1]) wird die Wahrscheinlichkeit eines dem Ramaneffekt analogen Prozesses, nämlich der Simultanemission zweier Lichtquanten, berechnet. Es zeigt sich, daß eine Wahrscheinlichkeit dafür besteht, daß ein angeregtes Atom seine Anregungsenergie in zwei Lichtquanten aufteilt, deren Energien in Summe die Anregungsenergie ergeben, aber sonst beliebig sind. Fällt auf das Atom Licht, dessen Frequenz kleiner ist, als die entsprechende Eigenfrequenz des Atoms, so tritt außerdem noch eine erzwungene Doppelemission hinzu, bei der das Atom seine Energie in ein Lichtquant der eingestrahlten und eins der Differenzfrequenz aufteilt. Kramers und Heisenberg[2]) haben die Wahrscheinlichkeit dieses letzteren Prozesses korrespondenzmäßig berechnet.

Außerdem wird die Umkehrung dieses Prozesses betrachtet, nämlich der Fall, daß zwei Lichtquanten, deren Frequenzsumme gleich der Anregungsfrequenz des Atoms ist, zusammenwirken, um das Atom anzuregen.

Ferner wird untersucht, wie sich ein Atom gegenüber stoßenden Teilchen verhalten kann, wenn es gleichzeitig die Möglichkeit hat, spontan Licht zu emittieren. Oldenberg[3]) findet experimentell eine Verbreiterung der Resonanzlinie des Quecksilbers, wenn er die angeregten Atome vielfach mit lang-

1) P. A. M. Dirac, Proc. of R. S. vol. **114**. S. 143 u. 710. 1927.
2) H. A. Kramers u. W. Heisenberg, Ztschr. f. Phys. 31. S. 681. 1925.
3) O. Oldenberg, Ztschr. f. Phys. 51. S. 605. 1928.

Fig. 1. First page of Maria Göppert-Mayer's article published by Annalen der Physik (Göppert-Mayer, 1931).

$$W^{(2)}_{i\to f} = \frac{1}{\hbar^4}\left|\int_0^t dt''\int_0^{t''} dt'\langle f|U_0(t,t'')V(t'')\times U_0(t'',t')V(t')U_0(t')|i\rangle\right|^2 \quad (6)$$

Since transitions are performed between the eigenstates of H_0, it is useful to write transition amplitudes in terms of them:

$$W^{(2)}_{i\to f} = \frac{1}{\hbar^4}\left|e^{-(i/h)E_f t}\sum_m\int_0^t dt''\int_0^{t''} dt' e^{i(E_f-E_m/h)t''}\times e^{i(E_m-E_i/h)t'}\langle f|V(t'')|m\rangle\langle m|V(t')|i\rangle\right|^2 \quad (7)$$

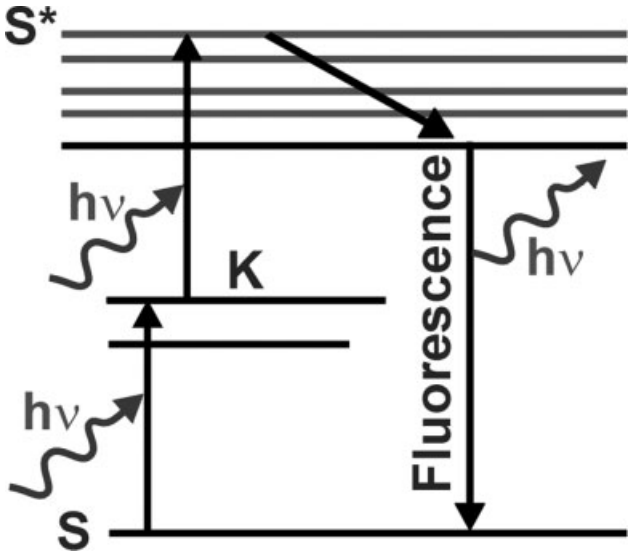

Fig. 2. Simplified scheme of the energy transition occurring under TPE regime.

where m are the intermediate virtual states for which $V_{mi} \neq 0$ and $V_{fm} \neq 0$.

The perturbing electric field felt by the fluorophore can be described by a constant operator C and a time-dependent factor:

$$V(t) = Ce^{-i\omega t}$$

where C, the max amplitude, is a vector that describes the polarization direction of light.

It is now convenient to introduce the Bohr frequency ω_{ab} and work under single intermediate level approximation:

$$\omega_{ab} = \frac{E_a - E_b}{h} \Rightarrow W^{(2)}_{i\to f} = \frac{|C_{fm}C_{mi}|^2}{\hbar^4\omega^2_{mi}} \times \left|\int_0^t dt'[e^{i\omega_{ni}t'} - e^{i\omega_{nmt'}}]\right|^2 \quad (8)$$

This represents a transition mediated by only one virtual level m. Two photons of suited energy have to interact simultaneously with the fluorescent dye to be absorbed and to excite it, according to the simplified Perrin-Jablonsky scheme shown in Figure 2.

Let C_{ab} be the matrix elements of the constant perturbation operator. In the Coulomb gauge, they can be written as

$$C = \frac{e}{c}\frac{\vec{p}}{m}\cdot\hat{\varepsilon}A_0 e^{i\vec{k}\cdot\vec{r}} \quad (9)$$

where A is the vector potential and ϵ the polarisation vector.

It is now possible to calculate the second order transition rate, introducing the harmonic temporal behaviour of the perturbation and considering the transition

rate for the symmetric intermediate level between the ground and excited state:

$$w_{i\to f}^{(2)} = \lim_{t\to\infty} W_{i\to f}^{(2)} = \frac{2\pi}{\hbar^4\omega^2}\,|C_{fm}C_{mi}|^2\delta(\omega' - \omega) \qquad (10)$$

where δ is the Kronecker's delta function.

On the other hand, the vector potential can be related to the radiation intensity by means of the Poynting vector (N):

$$I = |\bar{N}| = \frac{c}{4\pi}\,|\bar{E}\times\bar{B}| = \frac{\omega^2}{2\pi c}\,A_0^2 \qquad (11)$$

Substituting equations (9) and (11) in (10) we obtain:

$$w_{i\to f}^{(2)} \propto I^2 \qquad (12)$$

Equation (12) shows the proportionality between the second-order transition probability (two-photon absorption) and the square of radiation intensity. The lasers used for microscopy work in the TEM_{00} mode. The light intensity distribution of a laser beam orthogonal section can be approximated as a gaussian-lorentian distribution having cylindrical symmetry (Xu, 2002):

$$I(\rho, z, t) = \frac{2P(t)}{\pi w^2(z)}\,e^{-[2\rho^2/w^2(z)]}; \quad w(z) = w_0\sqrt{1+\left(\frac{z}{z_R}\right)^2} \qquad (13)$$

where ρ and z are, respectively, the radial and axial coordinates referred to the origin in the in-focus spot; w_o is the laser beam diameter in the focus plane; and z_R is the Rayleigh length.

Since the emitted fluorescence is proportional to the transition probability, equations (12) and (13) show that the intensity of emission falls along the optical axis as the fourth power of the focal distance:

$$F \propto z^{-4}. \qquad (14)$$

This is a first important result strictly connected to the capability of TPE optical sectioning. Figure 3 depicts the experimental situation.

This relation and the related experimental conditions are similar to the classical confocal selectivity and account for the intrinsic confocality of a two-photon microscopy. It is thus possible to collect information only from the focal plane by a point-to-point scanning over it and get a set of in-focus slices of the sample for a further 3D reconstruction. Figure 4 shows some TPE optical sections from a fluorescent object.

This spatial selectivity is achieved in the one-photon confocal microscopes by means of pinholes that reduce the out-of-focus emitted fluorescence. Despite this improvement of system performances, wider regions of the sample, compared to TPM, undergo laser excitation causing a high degree of photobleaching and photodamaging phenomena. Moreover, the confocal microscope is particularly sensitive to the laser alignment

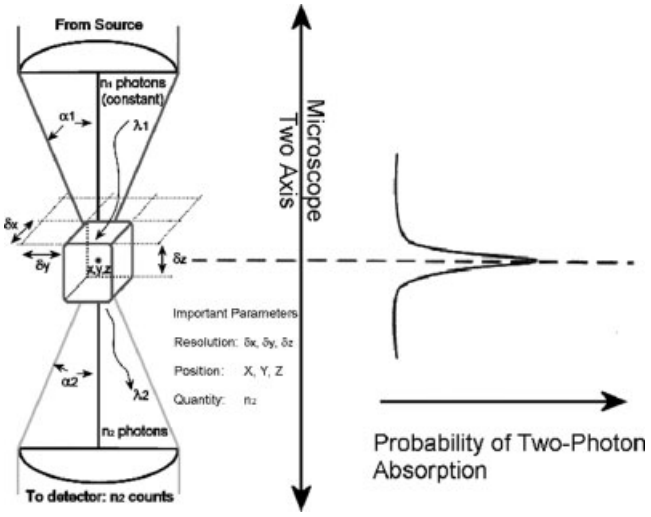

Fig. 3. Excitation optical pathway defining the volume of event for TPE fluorescence. Modified from Pawley's fundamental book (Pawley, 1995).

and a small pinhole leads to a worse signal-to-noise ratio because of the loss of signal.

CROSS-SECTION AND COLOCALIZATION

The proportionality factor in equation (12) can give further insights about the two-photon cross-section. It is possible to derive it under dipole approximation:

$$\begin{cases} e^{i\bar{k}\cdot\bar{r}} = 1 + \bar{k}\cdot\bar{r} + \cdots \approx 1 \\ \dfrac{\bar{p}}{m} = \dfrac{1}{i\hbar}\,[\bar{r}, H_0] \end{cases} \Rightarrow$$

$$w_{i\to f}^{(2)} \approx \frac{8\pi^3 e^4}{\hbar^4\omega^2 c^2}\,I^2|\langle f|\hat{\varepsilon}\cdot\bar{r}|m\rangle\langle m|\hat{\varepsilon}\cdot\bar{r}|i\rangle|^2\delta(\omega' - \omega) \qquad (15)$$

The first order approximation is a good one since $k = 2\pi/\lambda$ and $\lambda >> r$. Indeed a fluorophore is very small compared to the wavelength of light, and the spatial variation of the electric field within the molecule can be ignored.

Some constants can be grouped together in the fine structure constant and the radiation intensity divided by the single photon energy to get it in terms of number of photons:

$$w_{i\to f}^{(2)} \approx 8\alpha^2\pi^3|\langle f|\hat{\varepsilon}\cdot\bar{r}|m\rangle\langle m|\hat{\varepsilon}\cdot\bar{r}|i\rangle|^2\delta(\omega' - \omega)\left(\frac{I}{\hbar\omega}\right)^2 \qquad (16)$$

Furthermore, the two-photon cross-section can be written introducing again a sum over all the possible excitable intermediate levels:

$$\sigma_{TPE} \approx \sum_m 8\alpha^2\pi^3|\langle f|\hat{\varepsilon}\cdot\bar{r}|m\rangle\langle m|\hat{\varepsilon}\cdot\bar{r}|i\rangle|^2\delta(\omega' - \omega) \qquad (17)$$

On the other hand, the single-photon cross-section is expressed as (Sakurai, 1985):

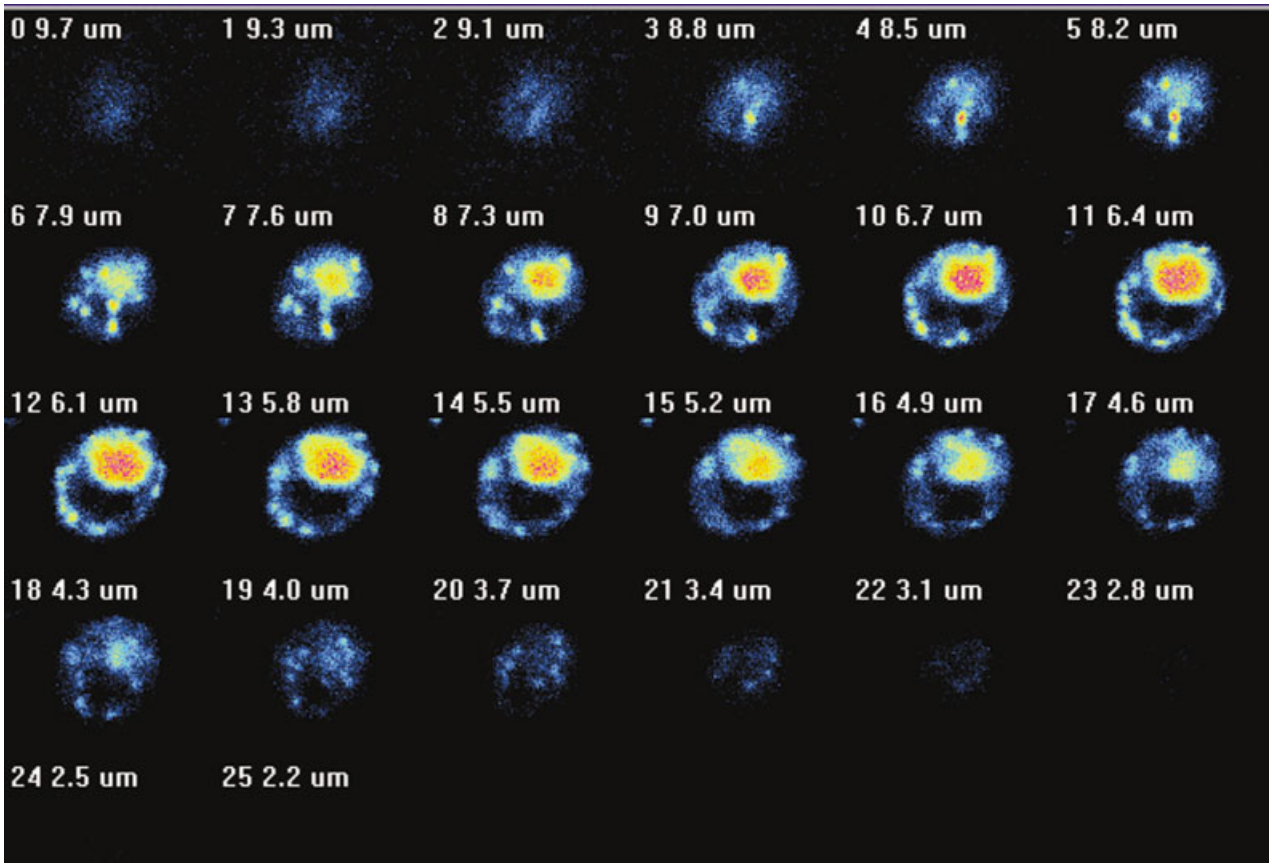

Fig. 4. Optical slices revealing DNA patterns in baker's yeast cell. TPE was performed at 780 nm. False digital colors are used. [Color figure can be viewed in the online issue, which is available at www.interscience.wiley.com.]

$$\sigma_{SPE} \approx 4\alpha\pi^2 |\langle f|\hat{\varepsilon}\cdot\vec{r}|i\rangle|^2 \omega\delta(\omega' - \omega) \tag{18}$$

In equation (18), the square of the matrix element gives the selection rules, ω the lifetime of the transition, and the delta-function is the ideal absorption spectra profile.

Comparing equations (17) and (18), we can outline the different selection rules and the same delta function profile but, in the former case, summed over an intermediate level set. Due to the different selection rules and to the sum over the different states, the experimentally observed two-photon cross-sections, if rescaled in a half-wavelength scale, are quite broader or at least equal to the single-photon one.

According to equations (17) and (18), TPE cross-section can also be written (Xu, 2002) as:

$$\sigma_{TPE} \approx \sum_m \sigma_{fm}\sigma_{mi}\tau_m \tag{19}$$

where single-photon cross-sections for transition *to and from* an intermediate level m are stressed together with its lifetime.

Broader cross-sections let more fluorescent dyes be simultaneously excited, so the choice of emission spectra whose overlap is negligible allows three-dimen-

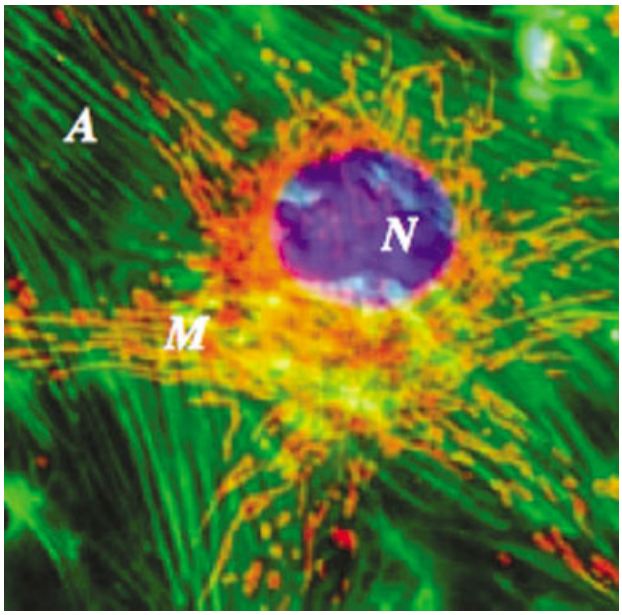

Fig. 5. Multiple fluorescence image. Nuclear DNA (N), mitochondrial distribution (M), and actin filaments (A) are visible after TPE at 720 nm. Sample is a bovine pulmonary artery endothelial cell (F-147780, Molecular Probes). [Color figure can be viewed in the online issue, which is available at www.interscience.wiley.com.]

sional distributions to be simultaneously recovered through TPE technique. Figure 5 shows an experimental consequence of this behaviour. In fact, a TMP can employ only one laser source for excitating multiple exogenous or endogenous fluorescent molecules; thus, it prevents any chromatic aberration during the excitation process. Furthermore, one can be fairly sure that the collected fluorescence mostly comes from the focal volume because of the extreme spatial selectivity of TPE. This causes chromatic aberrations to be as well negligible along the emission optical path, gaining a great improvement in colocalization experiments, due to the error minimisation in the estimate of reciprocal distances between different fluorescence distributions. On the contrary, in a single-photon confocal microscopy different laser lines are employed to excite different fluorescent dyes. Their spots are focused to different points inside the sample owing to lens chromatic aberration. Moreover, these same artefacts occur for the emitted fluorescence at different wavelengths. This all results in the loss of primary spatial dependence of the fluorescence intensity in the collected data that should undergo offline analysis to get more precise insights.

VIRTUAL TRANSITIONS AND LASER SOURCES

Two-photon microscopy takes advantages from virtual transitions that require the use of longer wavelength laser sources compared to single-photon excitation. However, the low cross-section of two-photon phenomena calls for a very high light power. Pulsed infrared or near-infrared lasers fit both these requests, for they allow a high enough peak power to observe two-photon absorption and a sufficiently low average power not to damage biological samples. In particular, radiation in the 700–1,000-nm wavelength range allows TPE of fluorescent dyes or samples whose single-photon absorption spectra are centred in the visible or ultraviolet wavelength range. This reduces radiation phototoxicity phenomena and lets conventional non-UV-adapted optics be employed. Moreover, it is worth pointing out that in the Lambert-Beer equation

$$I_{abs} = Ie^{\varepsilon Cl} \tag{20}$$

the molar extinction coefficient $\epsilon(\lambda)$ increases for shorter wavelengths; therefore, the use of longer wavelengths results in a grater penetration depth (de Grauw, et al., 2002). In equation (20), I_{abs} is the absorbed intensity, I the incident intensity, C is the dye concentration, and l the optical path length inside the sample.

All the TPM advantages outlined in this theoretical approach are reached at the cost of an overall loss of spatial resolution. Indeed, longer wavelengths result in a deterioration of resolution although the signal-to-noise ratio increase seems to balance this disadvantage.

EMITTED FLUORESCENCE DEPENDENCIES

The first counting of the number of photons per time unit absorbed at the focal plane under TPE was developed by Denk and co-workers (Denk et al., 1990). They referred to the following relationship for the emitted fluorescence:

$$F \propto \frac{\sigma_{TPE} P^2}{f_P \tau_P} \left(\frac{NA^2}{2\hbar c \lambda} \right)^2 C \tag{21}$$

where P, f_p, and τ_p are, respectively, the average power, the repetition rate, and the pulse duration of the laser, NA the numerical aperture of the objective, and C the dye concentration. The implicit approximation underlying this equation makes it useful for single molecule experiments as well as for a general comprehension of the phenomenon.

For thick samples, some integration over the sample volume is needed. According to Xu's calculations (Xu, 2002):

$$F \propto \frac{\sigma_{TPE} P^2}{2\lambda f_P \tau_P} n_0 C \tag{22}$$

The dependence by the fourth power of the objective numerical aperture NA is here absent. Indeed, the integration performed over spatial coordinates cancelled the dependence on geometrical parameters. Similar conclusions can be achieved by integrating over the focal volume (Hopt and Neher, 2001) defined by the microscopy resolution.

In what follows, the measured fluorescence intensity will be related to the fluorescent dye concentration and to the experimental parameters. For this reason, one more integration is performed over the signal integration period. The number of photons N_e emitted by the entire volume sample V is:

$$N_e = \int_V d\vec{r}\, \frac{1}{2}\, \phi_0 \sigma_{TPE} C(\vec{r}, t) I^2(\vec{r}, t) \tag{23}$$

where $\phi 0$ is the dye quantum yield, C the dye concentration in the sample, and I the laser beam intensity.

The light intensity distribution can be written as mathematical product of a time- and spatial-dependent part:

$$I(\vec{r}, t) = I_0(t) S(\vec{r}) \tag{24}$$

and the time-dependent term, in the paraxial approximation, can be expressed as:

$$I_0(t) = \frac{\pi NA^2}{\lambda^2} P(t) \tag{25}$$

It is possible to neglect the lack of homogeneity of fluorescent dye in the focal volume and use the mean-value theorem to integrate S^2:

$$N_e = \frac{1}{2}\, \phi_0 \sigma_{TPE} I^2(t) \int_V d\vec{r} c(\vec{r}, t) S^2(\vec{r}) \approx \frac{1}{2}\, \phi_0 \sigma_{TPE} I_0^2(t) C(t) \bar{S}\, \frac{\lambda^3 n_0}{NA^4} \tag{26}$$

where $\bar{S}$is a constant comprehensive of factors dependent on different focal volume definitions. Substituting equation (25) in (26):

$$N_e = \bar{S}\,\frac{\pi^2\phi_0\sigma_{TPE}}{2\lambda}\,n_0P^2(t)C(t) \tag{27}$$

The concentration position dependence due to the focal volume position in the sample is implicit in equation (27). The measured fluorescence intensity over a time integration period T, at time t and focusing the laser in the r position of the sample, is:

$$\langle F(t,\vec{r})\rangle_T \approx G\varepsilon(NA,\lambda)\cdot\bar{S}\,\frac{\pi^2\phi_0\sigma_{TPE}}{2\lambda}\,n_0\int_T dtc(t,\vec{r})P^2(t) \tag{28}$$

where ϵ is the acquisition channel efficiency and G represents a generic conversion factor or gain for the acquisition system.

Since the laser source is pulsed at a very high repetition rate f_p, the dye concentration can be regarded as constant during the single pulse but not over the total signal integration period:

$$\langle F(t,\vec{r})\rangle_T \approx G\varepsilon(NA,\lambda)\cdot\bar{S}\,\frac{\pi^2\phi_0\sigma_{TPE}}{2\lambda}\,n_0 \times\sum_i C(t_i,\vec{r})\int_{t_i-(1/2f)}^{t_i+(1/2f)} dtP^2(t) \tag{29}$$

Since light detectors measure average power, it is convenient to introduce the second order coherence (Xu, 2002) of the laser:

$$g = \frac{\langle P^2\rangle}{\langle P\rangle^2} = \frac{\xi}{f_P\tau_P} \tag{30}$$

where g is a source parameter and $\zeta = 0.66$ (for a typical TPM laser).

Finally:

$$\langle F(t,\vec{r})\rangle_T \approx GTP^2\varepsilon(NA,\lambda)\cdot\frac{\pi^2\phi_0\sigma_{TPE}g\bar{S}}{2\lambda}\cdot n_0\langle C(t,\vec{r})\rangle_T \tag{31}$$

Equation (31) shows how the system parameters contribute to the measured fluorescence intensity.

It is worth stressing here how only a few parameters are generally well monitored on a typical microscope. The others, such as the dye quantum yield, could be actually affected by local interactions. That is why special experimental care has to be considered when moving from qualitative imaging to quantitative observations (Chirico et al. et al., 2003; Mertz, 1998; Patterson and Piston, 2001; Zipfel et al., 2003; Zoumi et al., 2002).

CONCLUSION

We reported some theoretical passages related to mechanisms involved in two-photon excitation linking them to currently used experimental conditions. So far, these notes contain something lost in the day-to-day utilization of TPE or, in general, not available on the fingertips.

This is also intended to be a small and infinitely unpretentious homage to Maria Göppert-Mayer from Max Born's Göttingen, as recently reminded by Barry Masters in a superb collection of Multiphoton papers (Masters, 2002).

REFERENCES

Chirico G, Cannone F, Diaspro A. 2003. Single molecule photodynamics by means of one- and two-photon approach. J Phys D Appl Phys 36:1682–1688.

Denk W, Strickler J, Webb W. 1990. Two-photon laser scanning fluorescence microscopy. Science 248:73–76.

de Grauw CJ, Frederix PLTM, Gerritsen HC. 2002, Aberrations and penetration in in-depth confocal and two-photon microscopy. In: Confocal and two-photon microscopy: foundations, applications, and advances. Diaspro A, editor. New York: Wiley-Liss.

Diaspro A, editor. 1999. Two-photon microscopy. Microsc Res Tech 47:163– 212.

Diaspro A, editor. 2001. Confocal and two-photon microscopy: foundations, applications, and advances. Diaspro A, editor. New York: Wiley-Liss.

Diaspro A, Chirico G. 2003. Two-photon excitation microscopy. Adv Imag Elect Phys 126:195–286.

Göppert-Mayer M. 1931. Über elementarakte mit zwei quantensprüngen. Ann Phys Lpz 9:273–283.

Hopt A, Neher E. 2001. Highly nonlinear photodamage in two-photon fluorescence microscopy. Biophys J 80:2029–2036.

Loudon R. 1983. The quantum theory of light. Oxford: Oxford University Press.

Masters BR, editor. 2002. Selected papers on multiphoton excitation microscopy. Bellingham, WA: SPIE Milestone Series, SPIE Press.

Mertz J. 1998. Molecular photodynamics involved in multi-photon excitation fluorescence microscopy. Eur Phys J D 3:53–66.

Nakamura O. 1999. Fundamentals of two-photon microscopy. Microsc Res Tech 47:165–171.

Patterson GH, Piston DW. 2000. Photobleaching in two-photon excitation microscopy. Biophys J 78:2159–2162.

Pawley JB, editor. 1995. Handbook of biological confocal microscopy. New York: Plenum Press.

Periasamy A, Diaspro A. 2003. Multiphoton microscopy. J Biomed Optics 8:327–328.

Sakurai JJ. 1985. Modern quantum mechanics. The Benjamin/Cummings Publishing Company, Inc., Redwood, California.

Xu C. 2002. Cross-sections of fluorescence molecules in multiphoton microscopy. In: Confocal and two-photon microscopy: foundations, applications, and advances. Diaspro A, editor. New York: Wiley-Liss.

Zipfel WR, Williams RM, Christie R, Yu Nikitin A, Hyman BT, Webb WW. 2003. Live tissue intrinsic emission microscopy using multiphoton-excited native fluorescence and second harmonic generation. Proc Natl Acad Sci USA 100:7075–7080.

Zoumi A, Yeh A, Tromberg BJ. 2002. Imaging cells and extracellular matrix in vivo by using second-harmonic generation and two-photon excited fluorescence. Proc Natl Acad Sci USA 99:11014–11019.